Behavioral/Systems/Cognitive

Blood Oxygen Level-Dependent Signal Variability Is More than Just Noise

Douglas D. Garrett,[1,2] **Natasa Kovacevic,**[1] **Anthony R. McIntosh,**[1,2] **and Cheryl L. Grady**[1,2,3]

[1]Rotman Research Institute, Baycrest, Toronto, Ontario M6A 2E1, Canada, [2]Department of Psychology, University of Toronto, Toronto, Ontario M5S 3G3, Canada, and [3]Department of Psychiatry, University of Toronto, Toronto, Ontario M5T 1R8, Canada

Functional magnetic resonance imaging (fMRI) research often attributes blood oxygen level-dependent (BOLD) signal variance to measurement-related confounds. However, what is typically considered "noise" variance in data may be a vital feature of brain function. We examined fMRI signal variability during fixation baseline periods, and then compared SD- and mean-based spatial patterns and their relations with chronological age (20–85 years). We found that not only was the SD-based pattern robust, it differed greatly, both spatially and statistically, from the mean-based pattern. Notably, the unique age-predictive power of the SD-based pattern was more than five times that of the mean-based pattern. This reliable SD-based pattern of activity highlights an important "signal" within what is often considered measurement-related "noise." We suggest that examination of BOLD signal variability may reveal a host of novel brain-related effects not previously considered in neuroimaging research.

Introduction

Within functional magnetic resonance imaging (fMRI) research, much of what we understand about brain function is based on average brain activation patterns. Researchers typically compute within-subject average signals across a given time course to capture what is conceived as the most relevant brain activity (see "Mean" in Fig. 1). This approach is steeped in statistical and scientific traditions, in which a primary assumption is that central tendency reflects the most representative value in a distribution, and thus, "signal" within distributional "noise." However, no matter how the brain is measured, it is obvious that the brain's natural state is inherently variable (see "Variance" in Fig. 1) (Arieli et al., 1996; Miller et al., 2002; Laskaris et al., 2003; Neumann et al., 2003; Huettel et al., 2004; Faisal et al., 2008; McIntosh et al., 2008). Current evidence suggests substantial intrasubject variability in the blood oxygen level-dependent (BOLD) signal within and across testing sessions, but BOLD signal variance is often discounted as merely reflecting issues with task, image acquisition and preprocessing, statistical power, reliability, or other nuisance effects (Aguirre et al., 1998; Miller et al., 2002; Neumann et al., 2003; Huettel et al., 2004; Smith et al., 2005; Andrews-Hanna et al., 2007; Jones et al., 2008).

However, several other areas of research have examined directly the properties and unique functionality of variance, and suggest that by considering rather than ignoring variance, our ability to understand and predict several important phenomena can improve dramatically (Stein et al., 2005; MacDonald et al., 2006; Faisal et al., 2008). For example, recent EEG work shows that greater brain signal variability may indicate a more sophisticated neural system that can explore multiple functional states, yields more stable behavioral performance, and may be an important index of the cognitive capacity of the human brain (Ghosh et al., 2008; McIntosh et al., 2008). Although the concept of variability has not completely eluded fMRI research, no study to date has considered BOLD variance as a within-person measure with intrinsic theoretical and predictive meaning. Among the myriad contexts where one could investigate the effect and function of variability in BOLD signals, normal human aging is an appropriate starting point. In many respects, aging has become a model for examining generalized "noise" in both brain and behavior (Li et al., 2006; MacDonald et al., 2006, 2009; Hultsch et al., 2008). With regard to fMRI, however, age-related BOLD variability requires exploration. In the current study, we characterized BOLD variability with several novel questions in mind: (1) Can we find spatial patterns of BOLD variability, suggesting that this variability is more than just "noise" in the brain? If so, are older or younger brains more variable, or does the answer depend on brain region? (2) What are the similarities and differences between mean- and variability-based spatial patterns with age? (3) Does either BOLD mean or variability do a better job of predicting age? (4) Can we determine whether variability effects are due simply to confounds that influence the BOLD signal?

Received Oct. 16, 2009; revised Jan. 13, 2010; accepted Feb. 12, 2010.

D.D.G. was supported by a doctoral Canada Graduate Scholarship from the Natural Sciences and Engineering Research Council of Canada, the Sir James Lougheed Award of Distinction from Alberta Scholarship Programs, the Naomi Grigg Fellowship for Postgraduate Studies in Gerontology from Soroptimist International of Toronto, and the Men's Service Group Graduate Student Fellowship from the Rotman Research Institute, Baycrest. This work was supported by a Canadian Institutes of Health Research grant to C.L.G. (MOP14036) and A.R.M. (MOP13026), and a James S. McDonnell Foundation grant to A.R.M. C.L.G. was supported also by the Canada Research Chairs program, the Ontario Research Fund, and the Canadian Foundation for Innovation. We thank Laura Garrett for her helpful editorial suggestions, and Stephen Strother for insightful comments and expertise. D.D.G., N.K., A.R.M., and C.L.G. wrote the manuscript. D.D.G. and N.K. performed the analyses. D.D.G., N.K., A.R.M., and C.L.G. designed the study. A.R.M. and C.L.G. designed the task.

Correspondence should be addressed to Douglas D. Garrett, Rotman Research Institute, Baycrest, 3560 Bathurst Street, Toronto, Ontario M6A 2E1, Canada. E-mail: d.garrett@utoronto.ca.

DOI:10.1523/JNEUROSCI.5166-09.2010

 0270-6474/10/304914-08$15.00/0

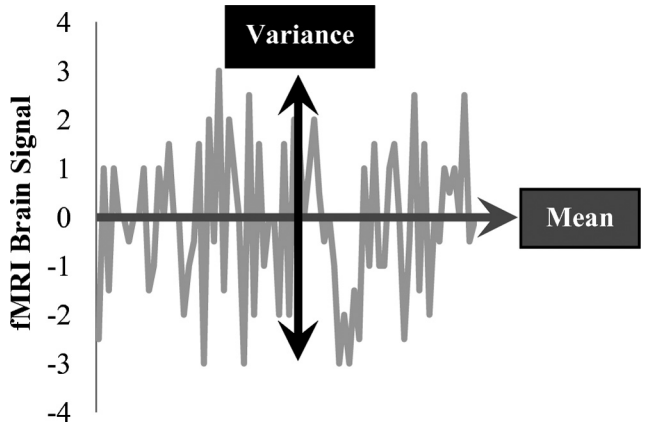

Figure 1. Conceptual comparison between fMRI signal mean and variability for a random brain voxel.

Materials and Methods

Sample

Our sample consisted of 19 young adults (mean age = 25.79 ± 3.28 years, range 20–30 years, 10 women) and 28 older adults (mean age = 66.46 ± 8.25 years, range 56–85 years, 14 women). Most participants were right handed (3 in each group were left handed), and all were screened using a detailed health questionnaire to exclude health problems and/or medications that might affect cognitive function and brain activity, including strokes and cardiovascular disease. Structural MRIs also were inspected to rule out severe white matter changes or other abnormalities. The young adults had significantly more years of education than did the older adults (young adults = 18.00 ± 2.10 years; older adults = 15.70 ± 3.10 years; $t_{(46)} = 2.80$, $p < 0.01$). There was no age difference in mean scores (mean scores for both groups = 29) on a test of mental status (Folstein et al., 1975). The present experiment was approved by the Research Ethics Board at Baycrest, and all participants gave informed consent for their participation (following the guidelines of the Research Ethics Board at Baycrest and the University of Toronto) and were paid for their participation.

Data of interest: fixation blocks

To maintain a simple model structure throughout, all mean and SD analyses were performed using only volumes acquired during fixation blocks from a broader study that also included several cognitive task blocks randomly interspersed (Grady et al., 2010). Participants viewed a fixation cross for the entirety of each block. On average, there were 32 fixation blocks per subject, with 10 volumes per block. This amounted to a total average of 320 volumes per subject (640 s of fixation) at a TR = 2000 ms.

fMRI scanning

We acquired images with a Siemens Trio 3T magnet. We first obtained a T1-weighted anatomical volume using SPGR (TE = 2.6 ms, TR = 2000 ms, FOV = 256 mm, slice thickness = 1 mm) for coregistration with the functional images and to ensure that there were no significant brain abnormalities in any participants. T2* functional images (TE = 30 ms, TR = 2000 ms, flip angle = 70°, FOV = 200 mm) were obtained using EPI acquisition. Each functional sequence consisted of twenty-eight 5-mm-thick axial slices, positioned to image the whole brain.

Data preprocessing

Common Template. For the purpose of creating an unbiased common anatomical template for a large age range (20–85 years), we first divided subjects into three age groups: 20–30, 55–65, and 66–85. For each of the three age groups, we created an unbiased nonlinear group average anatomical image (Kovačević et al., 2005; Chen et al., 2006; Levine et al., 2008). Starting with the three group-specific average images, we then applied the same algorithm to create a common anatomical image, which we refer to as the Common Template. The rationale behind this two-stage derivation of a Common Template was to accommodate large age differences across subjects. Brain anatomy changes significantly during normal aging (e.g., atrophy) (Ezekiel et al., 2004), and we assume that any individual subject registers better with subjects within the same general age group than with subjects from other groups. On the other hand, the three age-specific group average images are sufficiently blurry to allow easy coregistration. The transforms obtained from the two stages were concatenated to produce a single nonlinear transform from each subject into the Common Template space.

Table 1. Effects of preprocessing on BOLD signal variance and age prediction

Level of preprocessing	Voxel SDs	R^2 between SD brain and age	R^2 between mean brain and age
Basic	0.72 (0.48)	0.39	0.60
Extended	0.36 (0.20)	0.81	0.59

"Basic" preprocessing includes typical preprocessing steps (i.e., slice timing, motion correction, and spatial normalization and smoothing). "Extended" preprocessing includes independent components analysis, motion correction/white matter/cerebrospinal fluid parameter regression, and block normalization (see Materials and Methods). We calculated SDs over fixation blocks, and averaged them over brain and subjects. Between-subjects standard deviation of voxel SDs is given in parentheses. R^2 values represent proportion of variance accounted for in models where age was predicted separately by SD-based and mean-based brain scores.

Functional data. Functional data were slice-time corrected using AFNI (http://afni.nimh.nih.gov/afni) and motion corrected using AIR (http://bishopw.loni.ucla.edu/AIR5/) by registering all functional volumes to the 100th volume within run. By averaging all functional volumes within a motion-corrected run, we calculated mean functional volumes. For each run, mean functional volume was registered with each subject's structural volume using a rigid body transformation model. After appropriate transform concatenations, from initial volume to the 100th volume within run, from mean run volume to structural volume, and from structural volume into the Common Template space, we obtained a direct nonlinear transform from each initial fMRI volume into the Common Template space. We then applied the FSL/FNIRT registration algorithm to find a nonlinear transform between our anatomical Common Template and MNI 152_T1 provided with FSL software (www.fmrib.ox.ac.uk/fsl). Data were smoothed using an 8 mm Gaussian kernel. The steps outlined above comprised our "basic" preprocessing steps (i.e., slice timing and motion correction, spatial normalization, and smoothing) (Table 1).

We performed several additional preprocessing steps aimed at reducing data artifacts (termed "extended" preprocessing in Table 1). Functional volumes in the Common Template space were first corrected for artifacts via independent component analysis (ICA) within separate runs, as implemented in FSL/Melodic (Beckmann and Smith, 2004). Voxel time series were further adjusted by regressing out motion correction parameters, white matter (WM), and CSF time series. For WM and CSF regression, we extracted time series from unsmoothed data within small ROIs in the corpus callosum and ventricles of the Common Template, respectively. ROIs were selected such that they were deep within the each structure of interest (corpus callosum and ventricles) to avoid signal contamination from external tissues due to misregistration. The rationale for using small ROIs and unsmoothed data was to ensure that the ROIs would not contain any signal of interest (i.e., gray matter signal) for any of the subjects. The choice of a single 4 mm^3 voxel within corpus callosum for WM and a same-size voxel within one lateral ventricle for CSF was based on our experience in having excellent registration of these structures across all ages. With a large age span in our data, it would be easy to introduce age-related bias if larger ROIs or smoothed data were used. Spatial smoothing mixes signals from neighboring voxels on one hand, and registration errors during spatial normalization on the other; both factors can contaminate WM and CSF time series due to the close proximity of gray matter voxels. Although we used nonlinear registration to adjust for age related differences in anatomy (atrophy, in particular), it is still likely that residual differences remained such that, e.g., larger CSF ROIs would have residual small, yet biased, age-dependent contributions from GM signal.

To localize regions from our functional output, we submitted MNI coordinates to the Anatomy Toolbox in SPM8, which applies probabilistic algorithms to determine the cytoarchitectonic labeling of MNI coor-

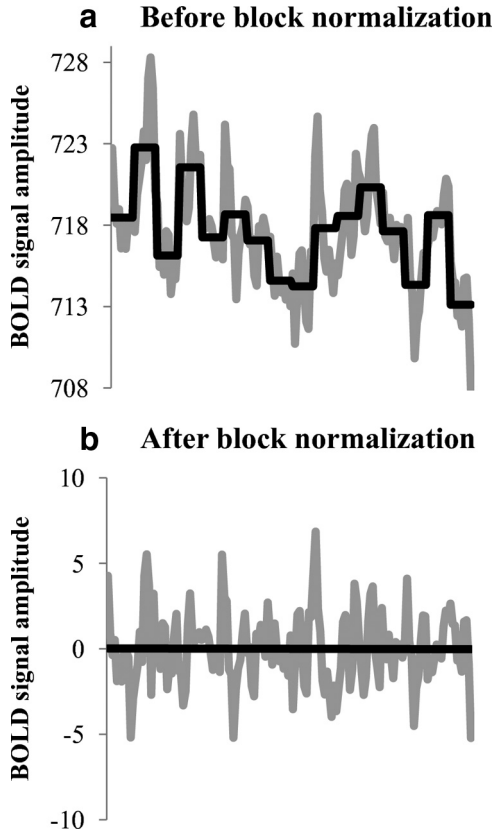

Figure 2. Example result of block normalization on a single voxel time series (shown in gray), obtained by concatenating 16 fixation blocks from two randomly selected runs (horizontal black lines represent mean block levels). Our experiment contained 32 blocks, but 16 are shown here for descriptive purposes, both before (***a***) and after (***b***) block normalization.

dinates (Eickhoff et al., 2005, 2007). Regions not labeled using this method were located manually using the Atlas of the Human Brain (Mai et al., 2008) after transforming MNI coordinates to Talairach space with the Nonlinear Yale MNI to Talairach Conversion Algorithm (Lacadie et al., 2008) and associated online Java-based applet. Supplemental Tables 1 and 2 (available at www.jneurosci.org as supplemental material) contain peaks of activation for SD- and mean-based measures for clusters comprised of at least 10 contiguous voxels, and associated peak bootstrap ratios of 3.00 or greater (for details, see Data analysis, Partial least-squares analysis of relations between BOLD SD and age, and BOLD mean and age).

Data analyses

Calculation of BOLD signal mean and SD. To calculate mean signal during fixation at each voxel, we first expressed each signal value as a percentage change from its respective block onset value, and then calculated a mean percentage change within each block (10 volumes per block) and averaged across all blocks (32 blocks, for a total of 320 volumes per subject). To calculate BOLD SDs during fixation, we performed an additional block normalization procedure. As an example, Figure 2*a* shows the time series from one voxel obtained by concatenating values across fixation blocks. We can see that large block offsets are present, likely due to residual low-frequency artifacts. To correct for this, we first normalized all fixation blocks such that the overall four-dimensional mean across brain and block was 100. For each voxel, we then subtracted the block mean and concatenated across all blocks (see Fig. 2*b* for an example). Finally, we calculated voxel SDs across this concatenated mean-block corrected time series.

Partial least-squares analysis of relations between BOLD SD and age, and BOLD mean and age. For each of the two fMRI signal measures, SD and mean, we performed separate partial least-squares (PLS) analyses (behavioral PLS) (McIntosh et al., 1996). PLS allows the identification of multivariate patterns of brain activity. This type of analysis begins with the correlation matrix between age and each voxel's signal, where correlations are calculated across subjects. The correlation matrix is decomposed using singular value decomposition (SVD) to produce latent variables, consisting of the correlation strength on one hand (i.e., the singular value), and a so-called "brain saliences" on the other (i.e., a weighting or loading pattern across brain voxels that optimally expresses the correlation). In the present study, because we had only one behavioral variable (age), only one latent dimension was possible for each PLS analysis. The effect of SVD in this simple case produces brain saliences that reflect the original voxelwise correlations with age, but are scaled to be unit length. We then calculated so-called "brain scores" (akin to component scores in principal component analyses) by taking the dot product of the brain saliences and a given subject's brain measures. Thus, in a single measure, a brain score indicates the degree to which a subject expresses the multivariate spatial pattern captured by an age-driven latent variable.

Significance of detected relations between multivariate spatial patterns and age was assessed using 1000 permutation tests of the singular value. A subsequent bootstrapping procedure revealed the robustness of voxel saliences across 1000 bootstrapped resamples of our data. By dividing each voxel's bootstrap mean salience by its SE, we obtained so called "bootstrap ratios" as normalized estimates of robustness. We thresholded bootstrap ratios at a value of 3.00, which is approximately equivalent to a 99% confidence interval.

Predicting age from mean- and SD-based brain scores. By construction, brain scores from the above analyses can be used to predict chronological age. Using each subject's mean- and SD-based brain scores, we examined joint and unique relations with chronological age using hierarchical linear regression. We emphasize that this statistical test was done to contrast the relative contributions of mean- and SD-based measures to the prediction of age, rather than to test the significance of prediction, which was done using 1000 permutation tests in the PLS analysis. We also performed an outlier analysis using Mahalanobis and Cook's distances following our regression model runs. Neither index revealed evidence for multivariate outliers in our data.

Effect of preprocessing on SD estimation, and its impact on relations with age. To illustrate the overall effects of preprocessing on our age-based variability effects, we first calculated average temporal signal variance across fixation scans within one run (run 1). To do so, for each brain voxel, we calculated the SD of the time series obtained by concatenating fixation blocks within the run. We then averaged the SD estimate across brain voxels and subjects. More extensive preprocessing yielded more conservative brain SD estimates, indicating we were successful in removing unwanted variance due to artifacts. To evaluate the statistical effect of successive preprocessing on the relations between SD brain and age, we calculated two multiple linear regression models, each regressing age onto SD brain scores calculated from basic and extended preprocessing steps. Similarly, we then evaluated the effect of preprocessing on the relation between mean brain and age (see Table 1). Our final results reported in the current study (in the first three sections of Results) reflect all preprocessing steps discussed in Table 1.

Results

Spatial patterns and age-related differences in BOLD variability

First, we examined the existence of age-related differences in voxel SDs. We used PLS (McIntosh et al., 1996) to calculate the presence and strength of multivariate spatial patterns of brain variability, and found a very strong relation with age ($R^2 = 0.81$, permuted $p < 0.0001$) (Fig. 3*a*). This relation was robust based on a bootstrapped estimated confidence interval (CI; 95% CI for $R^2 = 0.57, 0.93$). A robust pattern of voxels with age differences in BOLD SDs is shown in Figure 4*a*, with each voxel surpassing a bootstrap ratio threshold of 3.00 (approximating a 99% confidence interval; see Materials and Methods for further details). The bootstrapped pattern exhibited a distributed set of regions, including several that increased in variability with age (e.g., supe-

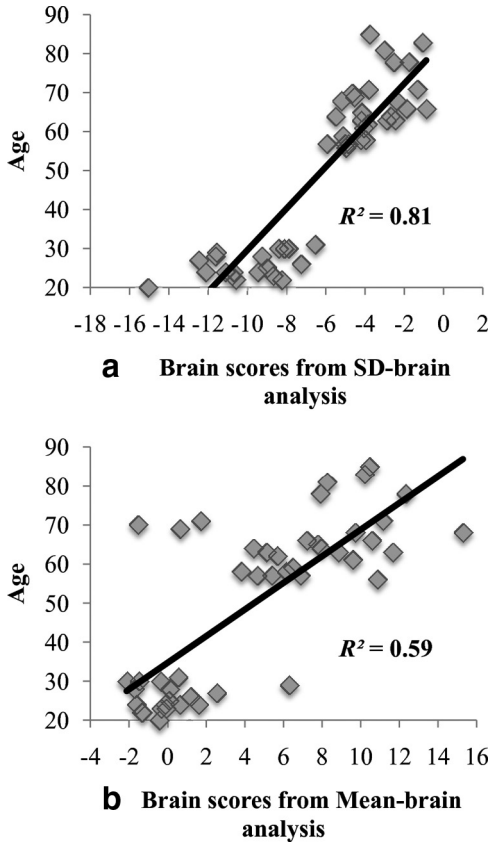

Figure 3. Zero-order relations between age and brain scores from SD- (***a***) and mean- (***b***) based analyses. We have deliberately used correlational analyses here, despite what appears to be an extreme group design. In initial model runs, we ran SD- and mean-based analyses with a dichotomous young/old variable, instead of a continuous measure of age. The use of dichotomous and continuous age variables yielded nearly identical results for each brain measure (within an R^2 of 1.00%). Thus, we elected to maintain the use of continuous age to allow better visualization of scatter around lines of best fit.

rior frontal gyrus, inferior temporal gyrus, cerebellum; shown in red), and many others that decreased in variability with age (e.g., lingual gyrus, middle temporal gyrus, supplementary motor area; shown in blue). This pattern suggests bidirectionality in voxel variability patterns; that is, although 33% of voxels increased in variability, the majority of brain voxels decreased in variability with age (67%). See supplemental Table 1 (available at www.jneurosci.org as supplemental material) for peak MNI coordinates, bootstrap ratios, and cluster sizes for each reliable cluster.

Similarities and differences between mean- and SD-based spatial patterns with age

Our mean-based PLS analysis also revealed a sizable relation with age ($R^2 = 0.59$, permuted $p < 0.0001$, 95% bootstrapped CI = 0.48, 0.62), but far less so than our SD-based results ($R^2 = 0.81$) (Fig. 3*b*). Bootstrap results revealed a multivariate pattern (Fig. 4*b*), including one area that increased (i.e., middle temporal gyrus; shown in red) and several that decreased in mean activity with age [e.g., superior parietal lobule, inferior temporal gyrus, inferior frontal gyrus (shown in blue); see supplemental Table 2 (available at www.jneurosci.org as supplemental material) for MNI coordinates, bootstrap ratios, and cluster sizes for reliable clusters]. Of critical importance in Figure 4, *a* and *b*, is that the mean- and SD-based patterns appear clearly distinct, which suggests that the two brain measures (mean and SD) revealed very different brain effects with age. To better characterize differences and similarities between these brain patterns, we computed overlay plots using only robust bootstrapped voxels (Fig. 4*c*,*d*). This analysis revealed remarkably different, virtually non-overlapping spatial patterns, despite the fact that mean- and SD-based measures were each highly related to age.

To quantify the lack of spatial overlap on a whole-brain level, we computed the dot product of mean- and SD-based brain saliences across all voxels and subjects (not just those voxels that surpass a bootstrap threshold of 3.00 or more); we then computed a bootstrapped 95% confidence interval around this dot product value. The dot product is equivalent to the cosine angle between two unit length vectors. Since brain saliences are unit length vectors by construction, the dot product can be taken as a similarity measure between mean- and SD-based saliences, with values ranging from −1.00 to 1.00. We found very weak spatial overlap (dot product = 0.11) between mean- and SD-based brain measures, with a bootstrap confidence interval that not only spanned zero, but remained weak at both ends (bootstrap CI = −0.25, 0.33). These results provide direct evidence that there is very little topographical overlap between age-based mean- and SD-brain patterns, and whatever overall similarity does exist is highly unreliable.

Which BOLD measure better predicts age?

Any conclusions about the utility of SD-based approaches rest partially on the ability of variance measures to add new information about the brain beyond that learned from assessing mean signals. Above, we found that spatial patterns using these two measures were markedly different, and that relations with age were stronger in our SD-based analyses. However, demonstrating the relative ability of each measure to predict age will better characterize unique contributions to modeling age-related brain differences. To do so, we extracted "brain scores" from the SD and mean-based analyses; these scores represented each participant's expression of the multivariate spatial pattern identified by each analysis. We then used both sets of brain scores (mean- and SD-based) to predict age using hierarchical linear regression. Our results revealed a sizable shared effect across both measures ($R^2 = 0.54$). However, mean-based brain scores revealed only a very small unique contribution to age ($R^2_{change} = 0.05$), whereas the unique contribution of SD-based brain scores to age was 5.19 times larger ($R^2_{change} = 0.27$) (Fig. 5). This suggests that our SD-based analysis yielded substantial predictive utility over and above mean-based effects.

There is a possibility that differences in predictive utility between means and SDs could reflect differences in measure reliability rather than validity (Schmiedek et al., 2009). To ascertain whether differences in reliability were present, we compared distributions of mean- and SD-based bootstrapped SEs for all voxels (total voxel count = 14,346; from our PLS analyses). We found that these distributions were virtually identical in both shape and central tendency (both with average SEs = ~0.14). Thus, the advantage in predictive power of our SD-based analysis is not attributable to differences in reliability between mean- and SD-brain measures.

Can we show that the SD-based measure is not unduly influenced by confounds that affect the BOLD signal?

Aging is associated with several possible confounds in fMRI data, the most notable of which includes various alterations in neurovascular coupling and vascular dynamics. Such confounds may yield a narrower dynamic range of BOLD signal responses, more

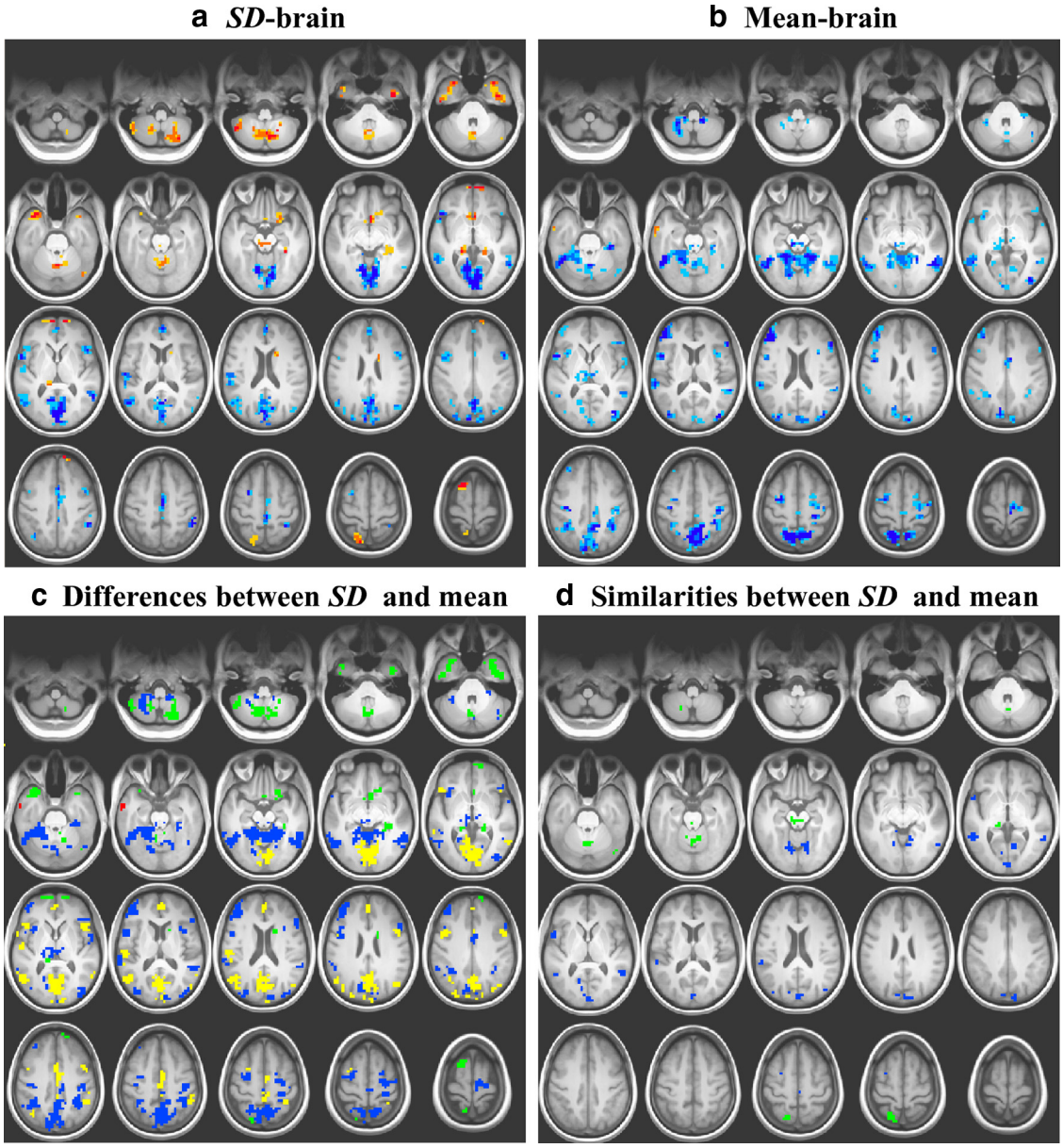

Figure 4. PLS brain patterns and overlay plots. ***a***, Yellow/red regions indicate robust age-related increases, and blue regions indicate age-related decreases, in BOLD SDs. ***b***, Yellow/red regions indicate robust age-related increases, and blue regions indicate age-related decreases, in BOLD means. In both ***a*** and ***b***, all robust areas surpassed a thresholded bootstrap ratio (salience/SE) of $\geq$3.00 (for yellow/red regions) or ≤ -3.00 (for blue regions). Darker colors indicate greater robustness. ***c***, Overlay plot highlighting differences between age-based SD- and mean-brain spatial patterns. Red, Mean increase, no SD effect; blue, mean decrease, no SD effect; green, SD increase, no mean effect; yellow, SD decrease, no mean effect. ***d***, Overlay plot highlighting similarities between age-based SD- and mean-brain spatial patterns. Blue, mean and SD both decrease with age; green, mean decrease, SD increase. All images represent every other slice in *z*-direction.

or less variable BOLD responses, and decreased signal-to-noise (Huettel et al., 2001; D'Esposito et al., 2003; Gazzaley and D'Esposito, 2005; Andrews-Hanna et al., 2007; Handwerker et al., 2007). Even though these (and other) confounds may affect any fMRI study of aging and are not easily controlled (D'Esposito et al., 2003; Gazzaley and D'Esposito, 2005; Handwerker et al., 2007), we argue against the substantial influence of these confounds on our variability-based results for two reasons. First, recent efforts to account for vascular confounds in fMRI research on aging assume these effects are essentially global (and thus unidirectional) in nature (Handwerker et al., 2007). However, the largely bidirectional pattern of age differences in variability seen in Figure 4*a* suggests that any "global" or unidirectional confound cannot account easily for our results. Second, if we are at risk of having "junk noise" drive our SD-based age effects (whatever the source), we should notice decreases in the ability of this measure to predict age with more extensive preprocessing. Importantly, we found that the opposite was true (see Table 1). After ICA denoising, white matter/CSF/motion parameter regression, and block normalization [which together reduced voxel SDs to 50% of the SD level found using more typical preprocessing steps (see Materials and Methods for a list of these steps)], the R^2 in age doubled, from 0.39 to 0.81. Conversely, mean-based relations were relatively unaffected by more extensive preprocessing ($R^2 = \sim$0.60 at most stages of preprocessing).

Discussion

In the current study, we attempted to characterize how variability in BOLD activity differs by age. First, we confirmed the presence of a robust age-related effect in a multivariate pattern of regions

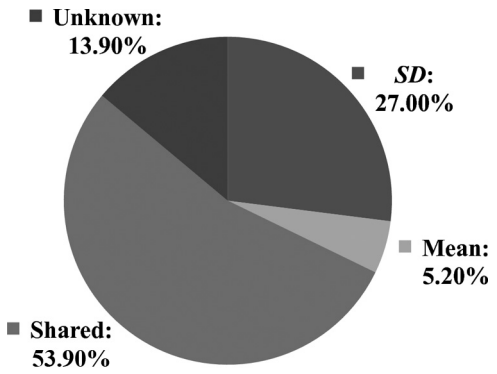

Figure 5. Relative contributions of SD- and mean-based brain measures for predicting chronological age. Values represent unique percentage variance accounted for (unique $R^2 \times 100$) in chronological age. "Shared" represents predictive overlap between mean- and SD-based measures; "Unknown" represents variance not accounted for by either mean- or SD-based measures. We found no interaction between the effects of mean and SD on age.

measured by BOLD variability. Notably, this suggests that spatial patterns exist across the brain when assessing what is typically considered "noise," and that these patterns can differentiate younger and older adults. We found also a bidirectional pattern of variability across regions, suggesting that age-related differences in variability are both spatially and directionally specific. Insofar as young adults represent an "optimal" system to which older adults can be compared, our bidirectional pattern suggests that even in young adults, variability is heterogeneous across the brain during fixation.

Second, we compared age-related SD- and mean-based multivariate patterns. Our mean-based PLS results revealed robust relations with age, but less so than for BOLD variability. Also, SD- and mean-based spatial patterns were essentially non-overlapping, despite the robust relation of each to age. This suggests that assessing the stability of the age-related BOLD signal reveals a highly distinct brain pattern not captured by mean-based approaches. Third, we expanded our comparison between SD- and mean-based measures to gauge unique variance accounted for in age. Examining BOLD variability would hold little value if it offered only marginal utility above that provided by the BOLD mean. Surprisingly, mean-based brain scores made only a very small unique contribution to age, whereas SD-based brain scores uniquely predicted age by more than five times the amount offered by the mean. This result should not be taken lightly. The zero-order mean-based effect was itself highly robust ($R^2 = 0.58$); however, simultaneously modeling the effect of SD-brain eliminated the majority of mean-based predictivity. We thus argue that, based on the combination of a distinct multivariate spatial pattern and heightened predictive ability, SD-based analyses may provide a novel window into the aging process. Further, although our results revealed a sizable shared relation between both brain measures and age ($R^2 = 0.54$), the brain regions identified by each measure were virtually non-overlapping at a robustness threshold of 3.00 or more. A dot product analysis using all voxels similarly revealed no reliable spatial overlap. It thus appears that even shared statistical relations between each measure and age (via our regression analyses) represent very different views of brain function.

Our final goal in the present study was to provide evidence that confounds that may influence the BOLD signal in older adults (and in general) cannot easily account for our findings. Although it is possible that global (and presumably unidirectional) vascular confounds may affect neurovascular coupling, vascular dynamics, and signal-to-noise ratios (D'Esposito et al., 2003; Gazzaley and D'Esposito, 2005; Handwerker et al., 2007), the bidirectional nature of our SD-based pattern suggests that such global confounds cannot render our effects untenable. In fact, far more voxels demonstrated reduced variability (67%) than increased variability (33%) with age, which argues against our result being due solely to an age-related decrease in "signal-to-noise" (see supplemental Table 1, available at www.jneurosci.org as supplemental material). As a more stringent test of the effect of various confounds, we also assessed the influence of preprocessing on the ability of mean and SD measures to predict age. We found that even though greater preprocessing substantially reduced voxel SDs (Huettel et al., 2004; Jones et al., 2008), the prediction of age dramatically increased to twice the level found when only basic preprocessing was applied. This suggests that greater age-related "signal" was revealed by voxel SDs as we removed further systematic sources of BOLD error variance. Based on these results, the removal of confounds may serve to further enhance, rather than reduce, SD-based age effects in future research.

What might brain variability reflect?

Several accounts offer insight into the dynamics and purpose of brain variability. Across a sample of children and young adults, McIntosh et al. (2008) found that greater multichannel EEG signal variability revealed a more sophisticated neural system that can explore multiple functional states. Importantly, the authors also found that signal variability was highly correlated with more consistent reaction time and more accurate performance, revealing an example of the potential real-world benefits of brain fluctuations. Others have suggested that substantial trial-to-trial brain variability derives from coherent spontaneous oscillations throughout the cortex (Laskaris et al., 2003; Fox et al., 2006; Nir et al., 2008). From this perspective, BOLD variability may reflect greater coherence between regions. Parga and Abbott (2007) found that under various conditions, neural networks can spontaneously and synchronously transition between up and down states. Interestingly, this ability is driven in part by a positive relation between excitatory and inhibitory membrane conductances; in a natural balance, excitation and inhibition may work together to produce neural function that is inherently variable. Notably, the authors also found that varying the external noise applied to such networks can modulate transitions between up and down states, thus enabling or inhibiting coherent fluctuations within a network.

Although such accounts help us conceptualize why greater variability in neural function is not simply noise, our bidirectional pattern suggests that older and younger adults differ in which regions demonstrate relatively higher or lower variability. If our young adults indeed represent an "optimal" system, a "sophistication" or "coherence" argument cannot easily account for areas where variability is less in young than in older adults (see red areas in Fig. 4*a*). Our older adults exhibited less variability overall, possibly reflecting less network complexity and integration, or greater white matter or synaptic loss that typifies the aging process (Sullivan and Pfefferbaum, 2006). However, what do we make of those regions where older adults exhibited more variability? Could these reflect compensatory processes that serve to counteract reduced network complexity and integration with age, or alternatively, could these reflect some form of dysfunctional signal variability? Stochastic resonance research suggests there is an optimal level of noise that facilitates neural function, and too little or too much noise results in a less efficient system

(Laurienti et al., 2006; Li et al., 2006; Parga and Abbott, 2007; Lugo et al., 2008; McDonnell and Abbott, 2009). Future work could address precisely to what "optimal" refers in an aging context.

Relatedly, another interesting computational account reflects exchanges between noise and neuronal output with age. Li et al. (2006) suggest that aging neurons produce less output per unit of input (so-called "gain"), and even the presence of ideal noise levels (yielding the benefits of stochastic resonance on signal detection) is not enough to overcome this neural inefficiency. The model of Li et al. (2006) also demonstrates that younger neurons require less noise to produce peak neural output, revealing a more efficient system. However, the authors used an external noise source to model the effects of SR with age. To the extent that internal noise sources may operate in a similar manner (i.e., producing the benefits of SR), their findings suggest that older neurons may benefit to some extent from internal variability, but not nearly to the same extent that young systems can. Should regions that show age-related increases in brain variability reflect a compensatory mechanism to counteract reduced neural efficiency with age, this may represent systemic efforts to induce SR-type benefits in the presence of neural inefficiency. Areas that show age-related decreases in BOLD SDs may then represent reductions in optimal variability levels with age (Fig. 4*a*).

Finally, it may simply be that greater variability is required naturally in some neural regions for optimal function, but not in others. Other researchers controlling for BOLD variability (as a confound) revealed that some regions show greater variability, some regions show reduced variability, and other regions show no difference across age groups (Andrews-Hanna et al., 2007). Perhaps spatially distinct variability is itself a proxy for the functional substrate of an "optimal" system, and only when optimal variability patterns are disrupted can age-related effects become evident.

Conclusion

BOLD variability exhibits a spatially coherent pattern, highly differentiates from the BOLD mean, and robustly relates to age. Representing a more dynamic view of brain function, examining BOLD variability is a novel approach that can be easily integrated into any fMRI research design. Given our results, we find no reason to simply consider BOLD variability as "noise." As Faisal et al. (2008) appropriately state, ". . . to understand the nervous system we have to distinguish variability from noise by accounting for its sources and appreciate the way in which it influences the brain's structure and function" (p. 300). Variance-based measures may in fact reveal a host of novel brain-related effects not previously considered in fMRI research, while simultaneously bridging to other research areas in which neural variability is expected and even functional (Stein et al., 2005; Faisal et al., 2008; McIntosh et al., 2008). Indeed, it seems that BOLD variability provides a new "signal" that deserves careful consideration.

References

Aguirre GK, Zarahn E, D'Esposito M (1998) The variability of human, BOLD hemodynamic responses. Neuroimage 8:360–369.

Andrews-Hanna JR, Snyder AZ, Vincent JL, Lustig C, Head D, Raichle ME, Buckner RL (2007) Disruption of large-scale brain systems in advanced aging. Neuron 56:924–935.

Arieli A, Sterkin A, Grinvald A, Aertsen A (1996) Dynamics of ongoing activity: explanation of the large variability in evoked cortical responses. Science 273:1868–1871.

Beckmann CF, Smith SM (2004) Probabilistic independent component analysis for functional magnetic resonance imaging. IEEE Trans Med Imaging 23:137–152.

Chen XJ, Kovacevic N, Lobaugh NJ, Sled JG, Henkelman RM, Henderson JT (2006) Neuroanatomical differences between mouse strains as shown by high-resolution 3D MRI. Neuroimage 29:99–105.

D'Esposito M, Deouell LY, Gazzaley A (2003) Alterations in the BOLD fMRI signal with ageing and disease: a challenge for neuroimaging. Nat Rev Neurosci 4:863–872.

Eickhoff SB, Stephan KE, Mohlberg H, Grefkes C, Fink GR, Amunts K, Zilles K (2005) A new SPM toolbox for combining probabilistic cytoarchitectonic maps and functional imaging data. Neuroimage 25:1325–1335.

Eickhoff SB, Paus T, Caspers S, Grosbras MH, Evans AC, Zilles K, Amunts K (2007) Assignment of functional activations to probabilistic cytoarchitectonic areas revisited. Neuroimage 36:511–521.

Ezekiel F, Chao L, Kornak J, Du AT, Cardenas V, Truran D, Jagust W, Chui H, Miller B, Yaffe K, Schuff N, Weiner M (2004) Comparisons between global and focal brain atrophy rates in normal aging and Alzheimer disease: boundary shift integral versus tracing of the entorhinal cortex and hippocampus. Alzheimer Dis Assoc Disord 18:196–201.

Faisal AA, Selen LP, Wolpert DM (2008) Noise in the nervous system. Nat Rev Neurosci 9:292–303.

Folstein MF, Folstein SE, McHugh PR (1975) "Mini-mental state." A practical method for grading the cognitive state of patients for the clinician. J Psychiatr Res 12:189–198.

Fox MD, Snyder AZ, Zacks JM, Raichle ME (2006) Coherent spontaneous activity accounts for trial-to-trial variability in human evoked brain responses. Nat Neurosci 9:23–25.

Gazzaley A, D'Esposito M (2005) BOLD functional MRI and cognitive aging. In: Cognitive neuroscience of aging (Cabeza R, Nyberg L, Park D, eds), pp 107–131. New York: Oxford UP.

Ghosh A, Rho Y, McIntosh AR, Kötter R, Jirsa VK (2008) Noise during rest enables the exploration of the brain's dynamic repertoire. PLoS Comput Biol 4:e1000196.

Grady CL, Protzner AB, Kovacevic N, Strother SC, Afshin-Pour B, Wojtowicz MA, Anderson JAE, Churchill N, McIntosh AR (2010) A multivariate analysis of age-related differences in default mode and task positive networks across multiple cognitive domains. Cereb Cortex. Advance online publication. doi:10.1093/cercor/bhp207.

Handwerker DA, Gazzaley A, Inglis BA, D'Esposito M (2007) Reducing vascular variability of fMRI data across aging populations using a breathholding task. Hum Brain Mapp 28:846–859.

Huettel SA, Singerman JD, McCarthy G (2001) The effects of aging upon the hemodynamic response measured by functional MRI. Neuroimage 13:161–175.

Huettel SA, Song AW, McCarthy G (2004) Functional magnetic resonance imaging. Sunderland, MA: Sinauer Associates.

Hultsch DF, Strauss E, Hunter MA, MacDonald SWS (2008) Intraindividual variability, cognition, and aging. In: The handbook of aging and cognition, Ed 3 (Craik FIM, Salthouse TA, eds), pp 2491–2556. New York: Psychology.

Jones TB, Bandettini PA, Birn RM (2008) Integration of motion correction and physiological noise regression in fMRI. Neuroimage 42:582–590.

Kovačević N, Henderson JT, Chan E, Lifshitz N, Bishop J, Evans AC, Henkelman RM, Chen XJ (2005) A three-dimensional MRI atlas of the mouse brain with estimates of the average and variability. Cereb Cortex 15:639–645.

Lacadie CM, Fulbright RK, Rajeevan N, Constable RT, Papademetris X (2008) More accurate Talairach coordinates for neuroimaging using non-linear registration. Neuroimage 42:717–725.

Laskaris NA, Liu LC, Ioannides AA (2003) Single-trial variability in early visual neuromagnetic responses: an explorative study based on the regional activation contributing to the N70m peak. Neuroimage 20:765–783.

Laurienti PJ, Burdette JH, Maldjian JA, Wallace MT (2006) Enhanced multisensory integration in older adults. Neurobiol Aging 27:1155–1163.

Levine B, Kovacevic N, Nica EI, Cheung G, Gao F, Schwartz ML, Black SE (2008) The Toronto traumatic brain injury study: injury severity and quantified MRI. Neurology 70:771–778.

Li S-C, Van Oertzen T, Lindenberger U (2006) A neurocomputational model of stochastic resonance and aging. Neurocomputing 69:1553–1560.

Lugo E, Doti R, Faubert J (2008) Ubiquitous crossmodal stochastic resonance in humans: auditory noise facilitates tactile, visual and proprioceptive sensations. PLoS ONE 3:e2860.

MacDonald SWS, Nyberg L, Bäckman L (2006) Intra-individual variability in behavior: links to brain structure, neurotransmission and neuronal activity. Trends Neurosci 29:474–480.

MacDonald SWS, Li S-C, Bäckman L (2009) Neural underpinnings of within-person variability in cognitive functioning. Psychol Aging 24:792–808.

Mai JK, Paxinos G, Voss T (2008) Atlas of the human brain, Ed 3. New York: Elsevier.

McDonnell MD, Abbott D (2009) What is stochastic resonance? Definitions, misconceptions, debates, and its relevance to biology. PLoS Comput Biol 5:e1000348.

McIntosh AR, Bookstein FL, Haxby JV, Grady CL (1996) Spatial pattern analysis of functional brain images using partial least squares. Neuroimage 3:143–157.

McIntosh AR, Kovacevic N, Itier RJ (2008) Increased brain signal variability accompanies lower behavioral variability in development. PLoS Comput Biol 4:e1000106.

Miller MB, Van Horn JD, Wolford GL, Handy TC, Valsangkar-Smyth M, Inati S, Grafton S, Gazzaniga MS (2002) Extensive individual differences in brain activations associated with episodic retrieval are reliable over time. J Cogn Neurosci 14:1200–1214.

Neumann J, Lohmann G, Zysset S, von Cramon DY (2003) Within-subject variability of BOLD response dynamics. Neuroimage 19:784–796.

Nir Y, Mukamel R, Dinstein I, Privman E, Harel M, Fisch L, Gelbard-Sagiv H, Kipervasser S, Andelman F, Neufeld MY, Kramer U, Arieli A, Fried I, Malach R (2008) Interhemispheric correlations of slow spontaneous neuronal fluctuations revealed in human sensory cortex. Nat Neurosci 11:1100–1108.

Parga N, Abbott LF (2007) Network model of spontaneous activity exhibiting synchronous transitions between up and down states. Front Neurosci 1:57–66.

Schmiedek F, Lövdén M, Lindenberger U (2009) On the relation of mean reaction time and intraindividual reaction time variability. Psychol Aging 24:841–857.

Smith SM, Beckmann CF, Ramnani N, Woolrich MW, Bannister PR, Jenkinson M, Matthews PM, McGonigle DJ (2005) Variability in fMRI: a re-examination of inter-session differences. Hum Brain Mapp 24:248–257.

Stein RB, Gossen ER, Jones KE (2005) Neuronal variability: noise or part of the signal? Nat Rev Neurosci 6:389–397.

Sullivan EV, Pfefferbaum A (2006) Diffusion tensor imaging and aging. Neurosci Biobehav Rev 30:749–761.